Analytical Biochemistry 696 (2025) 115693

Contents lists available at ScienceDirect

Analytical Biochemistry

journal homepage: www.elsevier.com/locate/yabio

Impact of Lectin biotinylation for surface plasmon resonance and enzyme-linked Lectin assays for protein glycosylation

Benjamin Serafin [a], Amine Kamen [b], Gregory De Crescenzo [a,**], Olivier Henry [a,*]

[a] Department of Chemical Engineering, Polytechnique Montreal, Montreal, QC, Canada
[b] Department of Bioengineering, McGill University, Montreal, QC, Canada

ARTICLE INFO

Keywords:
Surface plasmon resonance
Lectin
Biotin
Protein glycosylation
Streptavidin

ABSTRACT

Lectins are widely employed for the assessment of protein glycosylation as their carbohydrate binding specificities have been well characterized. In glycosylation assays, lectins are often conjugated with biotin tags, which interact with streptavidin to functionalize biosensing surfaces or recruit signal generating molecules, depending on the assay configuration. We here demonstrate that a high degree of biotin conjugation can limit total capture to streptavidin functionalized SPR surfaces due to multipoint binding, and can additionally bias the reported kinetic evaluations when measuring the interaction between lectins and glycoproteins by SPR. For microplate assays using different configurations, high biotinylation ratios can effectively amplify the signal obtained when using Streptavidin conjugates for detection, in some cases significantly lowering the limit of detection. The cumulative results express the importance of customizing the ligand biotinylation ratios for different assay configurations, as commercially obtained pre-biotinylated lectins are not necessarily optimized for different assay configurations.

1. Introduction

Glycosylation is a form of post-translational modification that occurs in all eukaryotic cells, and involves the attachment of polysaccharide chains, via the sequential addition of monosaccharides, to a protein. Glycosylation is not encoded by a protein's primary structure, but is instead the product of cellular glycosylation enzymes, which function in the endoplasmic reticulum (ER) and the Golgi apparatus [1]. Glycans play many biological roles, participating in glycoprotein folding, water solubility, protease resistance, in addition to cell-cell signaling, adhesion, trafficking, immune system activation, nutritional storage and more [2].

The monitoring of glycosylation is essential in the quality control of therapeutic proteins, especially in the case of monoclonal antibodies (mAbs). The identity of the glycans added to the mAbs impacts the overall conformation of the Fc domain, the affinity of their interactions with Fc receptors [3,4] and therefore the effectiveness of antibody-dependent cellular cytotoxicity (ADCC) and complement-dependent cytotoxicity (CDC) pathways [5]. Antibody glycosylation also affects their circulating half-life [6], and their potential to elicit adverse immune responses [6,7].

Due to their well-characterized sugar specificities, lectins are often used for the evaluation of protein glycosylation. Lectins are a class of non-catalytic sugar-binding proteins which participate in cell-cell signaling, adhesion and protein trafficking. In the immune system, lectins participate in pathogen recognition, regulation of the immune response and activation of the apoptotic pathway [8]. Lectins recognize glycans via their carbohydrate recognition domains (CRD). The selectivity of CRDs varies widely from lectin to lectin, with some showing rather broad range (specific to monosaccharides) and others being more narrow (specific to oligosaccharide chains with a defined sequence and specific linkages).

Lectins are employed in the enzyme linked-lectin assay (ELLA), a protein glycosylation assay derived from the enzyme linked-immunosorbent assay (ELISA). The ELLA does not require chemical or enzymatic modifications to the glycoproteins prior to analysis, and does not require any specialized equipment [9]. In ELLA assays, where the lectin replaces the primary antibody, it is common to conjugate the lectins with a universal label such as biotin, rather than use a specifically designed secondary antibody for each lectin in the assay [9,10].

* Corresponding author.
** Corresponding author.
E-mail addresses: gregory.decrescenzo@polymtl.ca (G. De Crescenzo), olivier.henry@polymtl.ca (O. Henry).

https://doi.org/10.1016/j.ab.2024.115693
Received 1 March 2024; Received in revised form 15 October 2024; Accepted 17 October 2024
Available online 19 October 2024

Another common approach for characterizing protein glycosylation employes surface plasmon resonance (SPR) biosensors. SPR biosensors are a powerful tool for the study of biomolecular interactions, as they provide information on the binding between two biomolecules in real-time, without the need for any label. Briefly, a biomolecule termed the ligand is covalently immobilized or reversibly captured to the sensor surface. A second biomolecule termed the analyte is then injected onto the surface and the binding of the analyte to the ligand is recorded in real-time to produce a sensorgram. SPR sensorgrams can be used to evaluate the affinity and kinetic constants of the ligand-analyte interaction, or for the determination of analyte concentration, depending on the conditions of the assay [11]. SPR has been widely employed to assess glycosylation, with lectins acting either as the immobilized ligand [12–17] or the injected analyte [18–21]. A common approach to the immobilization of lectins is the capture of biotinylated lectins to streptavidin-decorated surfaces.

For use in ELLA and many SPR assays, lectins are conjugated with biotin via covalent coupling. Covalent coupling of biotins to lectins is achieved via several chemical reactions, which can target amine, carboxyl or thiol functional groups present in amino acid side chains. Beyond selecting the target functional group, the chemical conjugation of biotin to proteins is random. Considerations should be taken to avoid coupling a biotin tag proximal to a protein's binding domain, as this could sterically hinder interactions with a second protein. The position of the biotin tag can be tightly controlled via the addition of an engineered biotin acceptor peptide (BAP) within the protein for BirA-mediated enzymatic conjugation [22]. Alternatively, cysteine residues [23] or aldehyde bearing amino acids [24] can be genetically engineered at specific locations in a protein to act as chemical handles for site-specific conjugation. While viable, these options are considerably more expensive, difficult and time consuming than chemical conjugation to naturally present side chains.

The biotin conjugation ratio plays an important role in the ELLA and SPR glycosylation assays. The ELLA uses streptavidin-HRP to produce a signal, and thus a high biotin to lectin ratio may amplify the signal strength for a given glycoprotein:lectin interaction (Fig. 1). In SPR, ligands with high biotinylation ratios achieve lower overall immobilization levels on streptavidin surfaces due to multipoint binding [25]. Additionally, a high biotin ratio at incubation is more likely to tag the lectins near their carbohydrate recognition domain, which can sterically hinder interactions or modify binding kinetics (Fig. 1). The biotin conjugation ratio of commercially available lectins is not provided by the manufacturers; it is thus impossible to estimate its impact upon assay performance. Conjugating lectins in-house would enable optimization of an otherwise uncontrolled variable.

In this work we explore the impact of biotin conjugation ratios on the performance of lectins in SPR assays and ELLA which employ the biotin-streptavidin interaction for surface capture or signal generation, respectively. To this end, three lectins; Lens Culinaris Agglutinin (LCA), Maackia Amurensis Lectin II (MAL-II) and Sambucus Nigra Agglutinin (SNA) were biotinylated to various degrees and applied to ELLA and SPR glycosylation assays, using model glycoproteins. Mannosylated rituximab (RTX) was used for D-mannose specific LCA. Bovine fetuin was used for both MAL-II and SNA, as it is known to bear both α2-3 and α2-6 linked sialic acids, for MAL-II and SNA respectively. Finally, we examined the performance of differentially biotinylated lectins and produce a decision matrix for the biotinylation approach of lectins, depending on the assay configuration and goal.

2. Materials

4 mL-capacity Amicon centrifugal filter units (molecular weight cut-off = 30 kDa) (#UFC8030), bicinchoninic acid (BCA) assay kit (#71285-3), phosphate buffered saline packs (#P5368), $MgCl_2$ (#M8266), Mn(II) Cl_2 (#244589), Tween 20 (#P7949), streptavidin (#189730), sulfuric acid (#258105) and TMB substrate (#T0440) were all purchased from Millipore Sigma. HEPES (#329850500) and $CaCl_2$ (#033296-A3) were purchased from Thermofisher. Streptavidin-HRP (#DY998) was purchased from R&D Systems. All lectins used in this study (LCA: #21510006, MAL-2: #21511098, SNA: #21510104) were purchased unconjugated from GlycoMatrix. The biotinylation reagent NHS-dPEG4-biotin was purchased from Quanta Biodesign Ltd. (#10200). Cysteine-tagged Kcoil and biotin-tagged Ecoil peptides (peptide sequences being CGG-$[KVSALKE]_5$ and CGG-$[EVSALEK]_5$, respectively) were chemically synthesized at the University of Colorado's peptide facility [26]. Ecoils were biotinylated at their terminal cysteine residue using biotin-maleimide, as described previously [27]. The Biacore T200 SPR biosensor, thiol coupling kit (#BR100557), HBS-EP buffer solution (#BR100669) and CM5 Series S sensor chips (#29149603) were purchased from Cytiva.

3. Methods

3.1. Lectin conjugation

Lectins were chemically conjugated using NHS-PEG4-biotin at a range of molar ratios: 0, 0.3, 1, 3, 10 and 30 mol of NHS-dPEG4-biotin per mol of lectin, diluted in 10 mM PBS (amine-free buffer solution). Lectins were incubated with the reagent for 30 min at room temperature (RT). Excess unreacted NHS-dPEG4-biotin (589 Da) was removed via

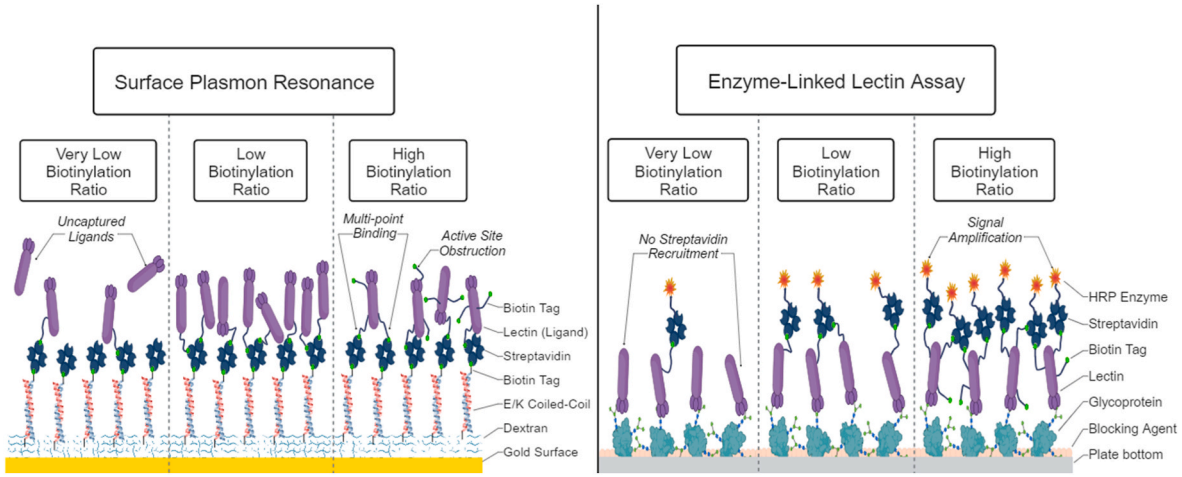

Fig. 1. Schematic illustration of the impact of the lectin biotinylation ratio on the performance of protein glycosylation assays using a surface plasmon resonance biosensor (left) or the enzyme linked lectin assay (right).

filter centrifugation (cut off = 30 kDa) for 5 cycles of 15 min at 3500 × g. The designation of the biotinylated lectins used throughout the study (R0, R0.3, R1, R3, R10 and R30) are derived from these incubation ratios.

Biotinylated lectins were quantified via the bicinchoninic acid (BCA) assay, using bovine serum albumin (BSA) and unconjugated lectin standards to construct a standard curve. The concentrations of all biotinylated lectins were thus adjusted for the remainder of the work, such that the only variable at play is the relative degree of biotin conjugation.

3.2. Relative biotinylation assay

The relative biotinylation assay was used to demonstrate the degree of lectin biotinylation resulting from each molar incubation ratio. Biotinylated lectins in PBS were directly incubated at 500 pM in a 96-well, flat-bottomed microplate. Traditional BSA blocking solutions could not be employed, due to the potential presence of contaminant glycoproteins within the BSA solution [9]. Instead, a protein-free blocking solution of 10 mM PBS containing 0.5 % v/v Tween (PBS-T) was used for all microplate assays [28]. Following the blocking step, the biotinylated lectins were detected using streptavidin-HRP and a TMB substrate solution, according to the manufacturer's instructions, and absorbance was measured at 450 nm. Absorbance levels were compared using a 1-tailed Student's t-test ($\alpha = 0.05$). Since the lectins were all incubated at the same concentration, the relative signal strengths are determined only by the biotin conjugation ratio.

3.3. ELLA assay

ELLA assays adopted the "direct" configuration, as reported in Ref. [9]. Model glycoproteins (rituximab for LCA, fetuin for MAL-II and SNA), for which the lectins have a well-documented specificity, were incubated overnight in the plate wells, which were then blocked with PBS-T. Biotinylated lectins diluted in a cation-containing buffer solution (10 mM HEPES buffer, pH 7.4, containing 150 mM NaCl, 1 mM $CaCl_2$, 1 mM $MgCl_2$, 1 mM $MnCl_2$ and 0.05 % Tween20) (HBS–I) were then added. Divalent cations such as Ca^{2+}, Mg^{2+}, Mn^{2+} and Zn^{2+} play an important role in lectin glycan binding through stabilization of the lectin CRD [29], and were therefore included in the buffer. To avoid signal saturation from an excessive number of biotins in the upper ranges of the assay, the concentration of Streptavidin-HRP was increased 2-fold from the manufacturer's instructions. Absorbance was again measured at 450 nm. Blank signals were obtained from wells containing no glycoprotein, which were otherwise treated the same. Each standard curve contained a blank signal produced with the appropriate lectin, which was subtracted from the other points in the curve.

The reported Limit of Detection (LOD) for each biotinylation ratio was calculated according to standard IUPAC guidelines (Equation (1)). The slope and blank were unique to each conjugation ratio. LOD were compared using a 1-tailed Student's t-test ($\alpha = 0.05$).

$$LOD_{Lectin} = \frac{Blank + (3.3 \times SD_{Blank})}{Slope} \quad \text{Equation 1}$$

3.4. Construction of a multi-capture streptavidin SPR surface

Regeneratable Kcoil decorated SPR sensor chips were constructed via thiol coupling, as previously reported [30]. Approximately 1500 RU of cysteine-bearing Kcoil were covalently immobilized to both the active and reference flow cells.

Regenerable streptavidin surfaces were produced anew at the start of each cycle using a multi-capture approach, ultimately anchored to the surface via the thiol coupled Kcoil [27]. First, 30 nM Ecoil-biotin was injected for 180 s and captured (~130 RU) by surface-bound Kcoil. Second, 250 nM streptavidin was injected for 30 s and captured (~500 RU) via its interaction with the biotin of the previously captured Ecoil. Third, biotinylated lectins were captured by the previously captured streptavidin (Fig. 2, left panel). At the end of the detection cycle, regeneration was achieved via five repeated pulses of 6 M guanidium-HCl, each lasting 30 s, to dissociate the stable and high-affinity Ecoil-Kcoil complex [31]. Following regeneration, only the Kcoil remained bound to the surface, and was available to capture biotinylated Ecoil for the next cycle. All injections were performed at 10 μL/min, aside from guanidium-HCl which was injected at 100 μL/min. Via targetetted regeneration at the site of the E/K coiled-coil interaction, we constructed over 300 such streptavidin surfaces to evaluate the capture of biotinylated lectin ligands.

Streptavidin and lectins were diluted in HBS-I, which served as the running buffer for all SPR experiments. To avoid aggregation via the formation of chelating ion bonds between negatively charged amino acid residues, the Ecoil-biotin was diluted in a buffer devoid of the divalent cation salts (i.e. HBS-EP).

3.5. Influence of biotinylation on capture kinetics

To evaluate how the biotin:lectin ratio affects the biotinylated lectin capture to a streptavidin surface, 100 nM of biotininylated lectins were injected onto a streptavidin surface for 8 min at 10 μL/min. Due to the very low dissociation rate of the streptavidin:biotin complex, the dissociation of the captured lectin is virtually null, especially for high conjugation ratios where rebinding is more likely to occur. All SPR sensorgrams were double referenced [11]: blank samples contained no lectins, whereas blank surfaces corresponded to surfaces where streptavidin was absent.

The lectin capture rate was derived from the quasi-linear initial portion of the association phase. Its slope, expressed in RU s^{-1}, was then divided by the concentration of the biotinylated lectin, leading to an initial capture rate expressed in RU s^{-1} M^{-1}.

3.6. Influence of biotinylation on binding kinetics

Kinetic titration experiments were performed to determine the impact of biotinylation on lectin-glycoprotein interactions. Herein, biotinylated lectins were immobilized to the biosensor surface via the multi-capture surface described previously. The model glycoproteins were injected at 10 μL/min for 300 s at four increasing concentrartions (long enough to reach equilibrium for each injection). Regeneration then followed. Again, all SPR signals were double referenced, though in this case blank samples contained no glycoproteins, and blank surfaces had no lectin captured.

Kinetic titration sensorgrams were analyzed by Scatchard analysis to estimate the thermodynamic association constant [32]. To reduce bias induced by experimental noise (0.5–1.5 RU), the steady state value (R_{eq}) was calculated by taking an average of the signal at equilibrium. (Fig. 3).

4. Results and discussion

4.1. Biotin conjugation levels produced by the different incubation conditions

Lectins were incubated at a range of molar ratios with biotin-PEG4-NHS, including 0, 0.3, 1, 3, 10 and 30 mol of biotin reagent per mole lectin. To evaluate the degree of biotin conjugation at the different molar incubation ratios, the lectins were adsorbed in multi well plates and their biotin tags were detected using streptavidin-HRP. In Fig. 4, we report the relative biotinylation levels (in arbitrary absorbance units) for the three lectins (LCA, MAL-II and SNA), at each biotin reagent-to-lectin molar ratio.

For all three lectins, increasing the incubation ratio produced a higher final biotin conjugation level, as evidenced by a greater absorbance signal. Each threefold increase in conjugation resulted in a statistically significant increase in absorbance, as measured using

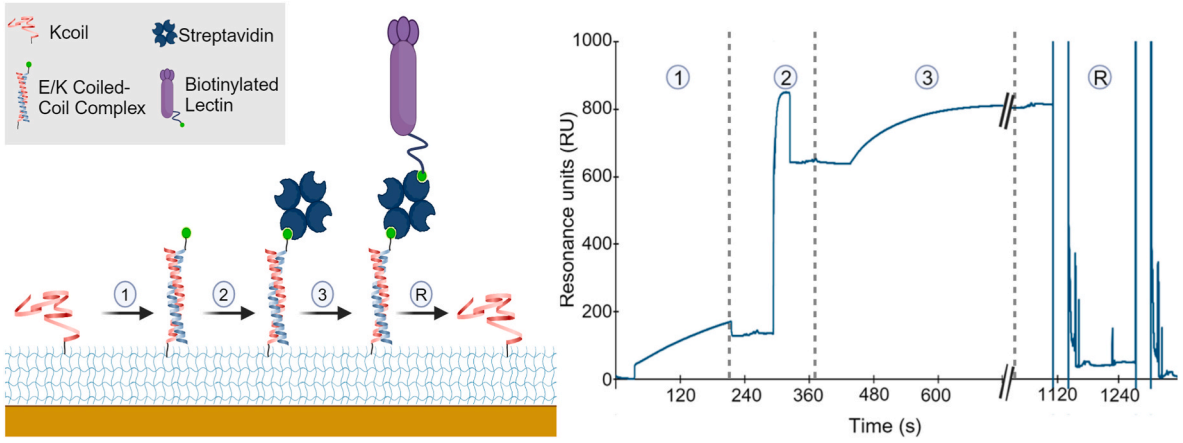

Fig. 2. Left: Schematic representation of the multi-capture streptavidin surface. Right: The associated sensorgram. At the beginning of the cycle, only the thiol coupled Kcoil is present at the surface. (1) Biotinylated Ecoil capture via coiled-coil interactions. (2) Streptavidin capture by the exposed biotin. (3) Capture of a biotinylated lectin by streptavidin, which acts as a linker for biotinylated biomolecules due to its homo-tetrameric quaternary structure. (R) Regeneration at the level of the coiled-coil interaction, leaving behind the thiol coupled Kcoil for the next capture cycle.

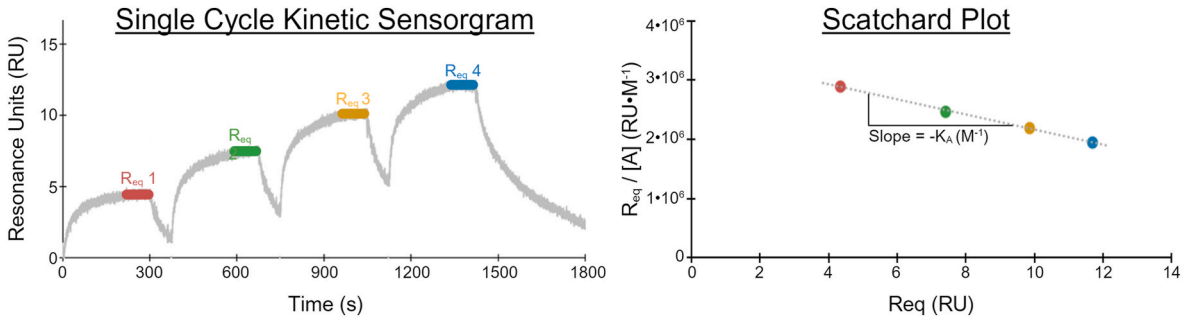

Fig. 3. Titration protocol for the interaction between immobilized MAL-II (R1) and injected fetuin. Titration sensorgram (Left panel) corresponds to fetuin injections at 1.5 μM, 3 μM, 4.5 μM and 6 μM. The signal at equilibrium (R_{eq}) is used to construct the Scatchard plot (Right panel).

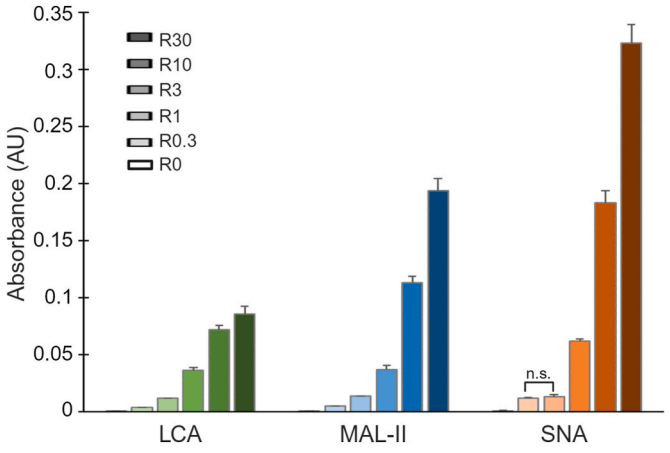

Fig. 4. Qualitative display of the relative biotin conjugation level produced by the various incubation conditions. For all three lectins, increasing the biotin-to-lectin molar ratio upon incubation produced significantly greater absorbance values, with the exception of R0.3 and R1 for SNA (α = 0.05) (n = 3).

streptavidin-HRP. The only exception was between R0.3 and R1 for the SNA lectin. Since all lectins were incubated at the same concentration, the only variable which contributed to the signal amplification was the number of biotin tags conjugated to the lectins.

While not the subject of the study, we also observed that the absolute signal produced by the different lectins varied. At the highest incubation ratio R30, the signal from SNA is 3.8-fold greater than that from LCA and 1.7-fold greater than that from MAL-II for the same incubation conditions. According to available primary sequence data, the three lectins contain a similar number of lysine residues (potential conjugation sites) per unit (LCA: 26 [33], MAL-II: 28 [34] and SNA: 26 [35]). The observed differences in signal amplitude more likely results from differences in lysine side chain availability within each lectin quaternary structure.

In this work, we did not quantify the absolute number of biotin tags conjugated in each incubation condition. While such an evaluation is possible via the HABA assay, this approach was unsuitable as the HABA limited by low-sensitivity and does not allow the recovery of analyzed samples [36]. Instead, the relative biotinylation assay presented here is a measure of functional biotinylation, which represents how the incubation conditions would influence the eventual biotin-streptavidin interactions, independent of lectin-glycoprotein interactions. Furthermore, it requires very little sample and no additional reagents (beyond those required for ELISA/ELLA style assays).

4.2. Biotin conjugation ratio impacts the kinetics of capture streptavidin surfaces

To evaluate the influence of the conjugation ratio on the capture kinetics, we injected lectins biotinylated at multiple incubation ratios onto a streptavidin surface and recorded the capture over time. These ratios were 0.3, 1, 3, 10 and 30 mol of biotin-PEG4-NHS per mole lectin, denoted as R0.3, R1, R3, R10 and R30 respectively. Fig. 5a presents the initial capture rate over the first 10 s of association (in $RUs^{-1}M^{-1}$). For the 3 lectins (LCA; green, MAL-II; blue, SNA; orange), we observe that

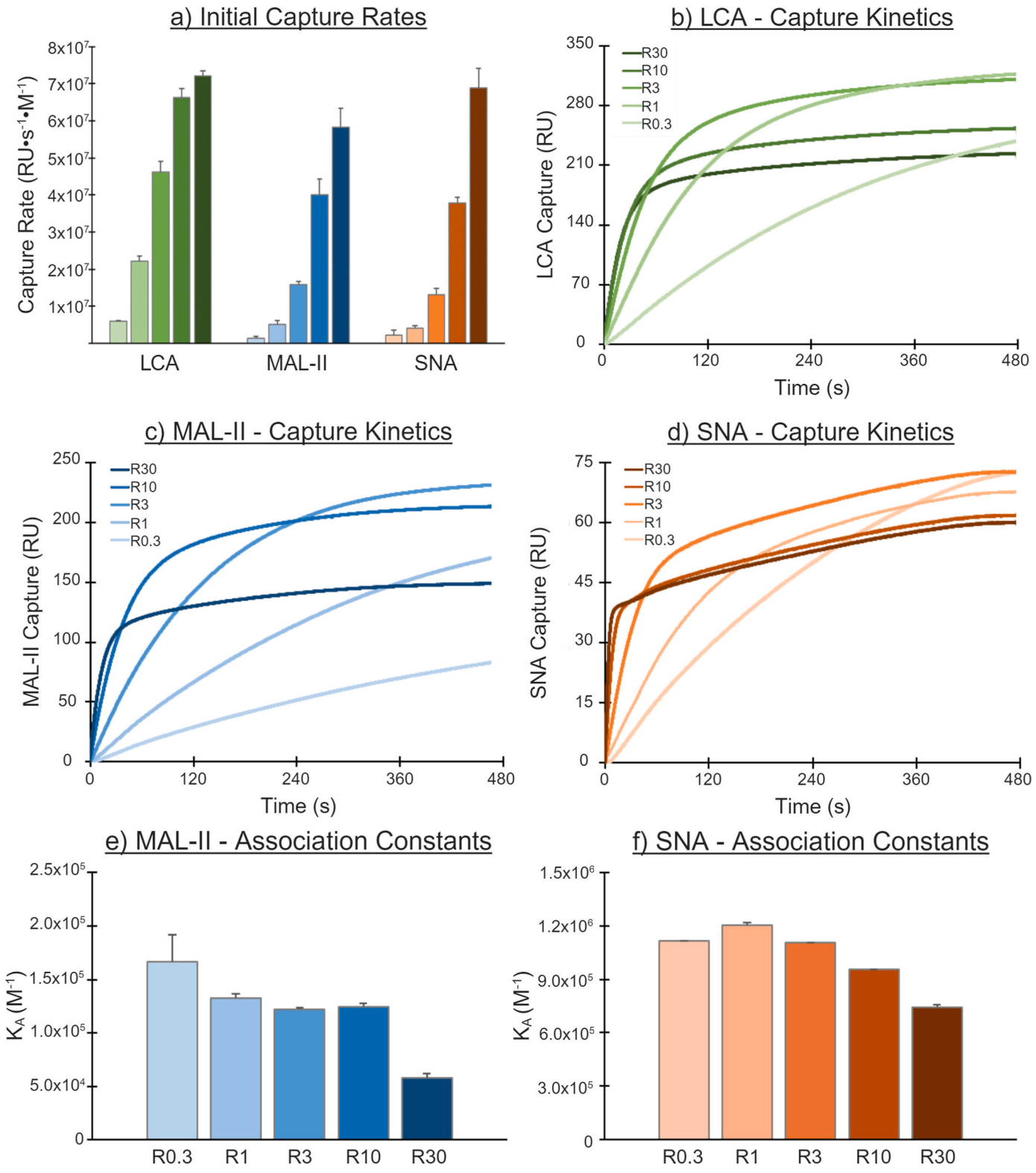

Fig. 5. a) Capture rates for biotinylated lectins on a streptavidin decorated SPR surface during the first seconds of the biotinylated lectin injection, calculated from the capture kinetics sensorgrams (n = 6). b, c, and d) SPR sensorgrams displaying LCA, MAL-II and SNA biotinylated to varying degrees being captured on a streptavidin decorated SPR surface (n = 6). e, f) Thermodynamic association constants of MAL-II and SNA, biotinylated to varying degrees, binding to injected Fetuin (n = 3).

the capture rate is faster for the higher conjugation ratios, indicating that the degree of biotinylation impacts the kinetics of the biotinylated lectin – streptavidin interaction. The amount by which the capture rate increases is more significant at lower ratios (i.e., between R0.3 and R1) than between higher ratios (i.e., between R10 and R30).

Fig. 5b, c and d depict the whole capture sensorgrams of the biotinylated LCA, MAL-II and SNA, in RU, over the entire 8 min injection period. For all 3 lectins, the higher ratios R10 and R30 achieve relatively

low capture amounts compared to the lower ratios. The lower ratios achieve greater capture, despite having slower associations, as depicted in Fig. 5a. The biotinylated lectin capture to streptavidin was functionally irreversible (Fig. S1). The lack of a dissociation curve is due to the remarkably strong interaction affinity of biotin and streptavidin [37], and due to a high density of streptavidin on the surface, which promotes rebinding [38].

The diminished capture levels observed at higher conjugation ratios are a demonstration of multipoint binding: a single lectin bearing multiple biotin tags binds to multiple streptavidin sites, and thus prevents the further capture of biotinylated lectins (as schematized in the High biotinylation ratio panel, Fig. 1). As a result, the total capture achieved on the surface is limited. While the lower conjugation ratios exhibit slower association (Fig. 5a), the streptavidin surface has a greater capacity over time, and the lower ratios display a higher capture over long injection periods. This is demonstrated by the capture sensorgrams of the 3 lectins (Fig. 5b, c and d) which show that the lower ratios R0.3 and R1) had not yet reached equilibrium after an 8-min injection.

The behaviours of the biotinylated lectins at the various biotinylation ratios present an interesting choice when preparing a biotin-streptavidin SPR surface. If low to moderate immobilization levels are desired (eg, lectin screening experiments), it would be preferable to use high conjugation ratios, which would reduce assay time and lower sample consumption. On the other hand, low conjugation ratios should be employed if high immobilization levels are desired (eg, for glycoprotein quantification studies) [11].

4.3. Excess biotinylation interferes with lectin-glycoprotein binding

The influence of excessive biotin conjugation on the affinity of the lectin-glycoprotein interactions was then evaluated. We injected the glycoprotein Fetuin, which bears glycans terminated by both α2-3 and α2-6 linked sialic acids, onto surfaces of MAL-II and SNA (α2-3 and α2-6 linked sialic acid specific, respectively) biotinylated at multiple conjugation ratios. The resulting lectin-glycoprotein interactions were recorded over time and the resulting titration sensorgrams were used to determine the thermodynamic affinity constants (K_A). The K_A for the lectins at each conjugation ratio are presented in Fig. 5e and f.

For MAL-II, we observe that R30 exhibits a significantly lower affinity for the glycoprotein analyte compared to the lower conjugation ratios (Fig. 5e). Going from R10 to R30 produces a sudden 54 % reduction in the calculated K_A, from $1.25 \times 10^5\ M^{-1}$ to $5.78 \times 10^4\ M^{-1}$, respectively. For MAL-II the lower conjugation ratios (R1, R3 and R10) exhibit very similar glycoprotein binding affinity.

For SNA, we instead report a more progressive reduction in binding affinity as the biotinylation ratio increases (Fig. 5f). Over the same interval of R10 to R30, a 22 % reduction in affinity is noted, from $9.55 \times 10^5\ M^{-1}$ to $7.45 \times 10^5\ M^{-1}$. For both lectins, the greatest loss in affinity is observed between R10 and R30. The greater affinity of SNA for fetuin, compared to MAL-II, is consistent with previous findings [39,40].

Results from lectin-glycoprotein binding experiments indicate that low biotinylation ratios are preferable for thermodynamic binding analysis, more likely as a result of biotin tags near the lectin CRD hindering glycoprotein binding (Fig. 1, see High biotinylation ratio panel for SPR).

4.4. High biotinylation ratio improves performance of the ELLA assay

To evaluate the impact of the biotin conjugation ratio on lectins in the ELLA, we compared standard curves of glycoprotein concentration constructed using each lectin at different biotinylation ratio. The signal for each glycoprotein concentration was measured in absorbance units, which is function of the streptavidin-HRP recruited by the lectins (Fig. 6a–c and e). The measured signal represents both the signal amplification produced by the increased biotinylation and the potential inhibition of lectin-glycoprotein binding caused by obstructive tagging. Due to the configuration of the assay, the influence of biotinylation on both these interactions (i.e., lectin-glycoprotein and biotin-streptavidin) could not be separated within the ELLA signal, as was possible with the SPR assays. The results derived from the standard curves are thus a representation of overall ELLA performance.

The trends are similar for all three lectins in the study. At lower conjugation ratios (R0.3-R3), we observe a signal amplification as we increase the biotin conjugation, exemplified by the steeper standard curves. This was also observed for the higher ratios (R10-R30), though the amplification was attenuated, as evidenced by the smaller differences between the standard curves, despite evidence of significant differences in biotin conjugation (Fig. 4). Reduced signal amplification at higher ratios is likely due to greater blank signals for these higher ratios, which was subtracted from the raw absorbances to correct for non-specific adsorption.

An important exception to this trend are the curves of R10 and R30 for MAL-II (Fig. 6c), for which no significant amplification of the signal was observed, despite a higher degree of biotin conjugation between these lectin preparations (Fig. 4, last two blue columns). Since the ELLA relies on lectin-glycoprotein binding (Fig. 1, see ELLA), the amplification effects due to high biotin conjugation (Fig. 4) is balanced by the reduction in binding affinity at these higher conjugation ratios (Fig. 5e and f). There is therefore a limit of effectiveness with respect to highly-biotinylating lectins for ELLA. The unique behavior of MAL-II, compared to the other lectins, can likely be attributed to the unique distribution of conjugation sites (i.e., solvent-exposed amine functional groups) on the protein. Depending on the proximity of these residues to the active binding domain, biotin-tags will have a variable effect on overall bioactivity. This is likely the cause for the variations between the relative biotinylation assay results (Fig. 4) and the ELLA results (Fig. 6) between the different lectins in this study.

The limits of detection (i.e., the lowest glycoprotein concentration that can be reliably detected) were calculated from these standard curves (Fig. 6b–d and f). The limit of detection was significantly higher, in all cases, for R0.3. In theory, we expect the limit of detection to decrease as the slope of the standard curve becomes steeper (Equation (1)). However, results show that at higher conjugation ratios, the LOD was not always significantly smaller for higher conjugation ratios (R3 vs. R10 for LCA, R3 vs. R10 vs. R30 for MAL-II, R10 vs. R30 for SNA). Two factors are likely responsible for this unexpected result: (*i*) blank sample noise is greater for high conjugation ratios, increasing the LOD (Equation (1)) and (*ii*) a reduced lectin-glycoprotein binding affinity (Fig. 5e and f) results in less lectin attachment, and therefore a signal amplification that is disproportionate to the increased biotin conjugation ratios. These observations suggest that excessive lectin biotinylation can effectively raise the limit of detection and impair the performance of the ELLA.

5. Conclusion

Results from SPR and ELLA assays demonstrate that the appropriate biotinylation ratio can significantly impact the performance of glycoanalytical assays (Fig. 7). Comparison of capture kinetics at varying biotinylation ratios, measured by SPR, indicates that lower ratios are capable of higher capture levels, as the inhibitory effects of multipoint binding are reduced. This would enable greater lectin immobilization, which would be advantageous for quantification assays. On the other hand, high conjugation ratios demonstrate a much faster association to a streptavidin surface, which would be advantageous for low to moderate capture levels, as it would reduce sample consumption and assay time.

ELLA assays have demonstrated an overall superiority of high biotinylation ratios, which produce significant signal amplifications and lower the limit of detection. This would be especially useful in the detection of very low glycoproteins concentrations, as in diagnostic settings. The limits of quantification would also be effectively reduced by increasing conjugation ratios.

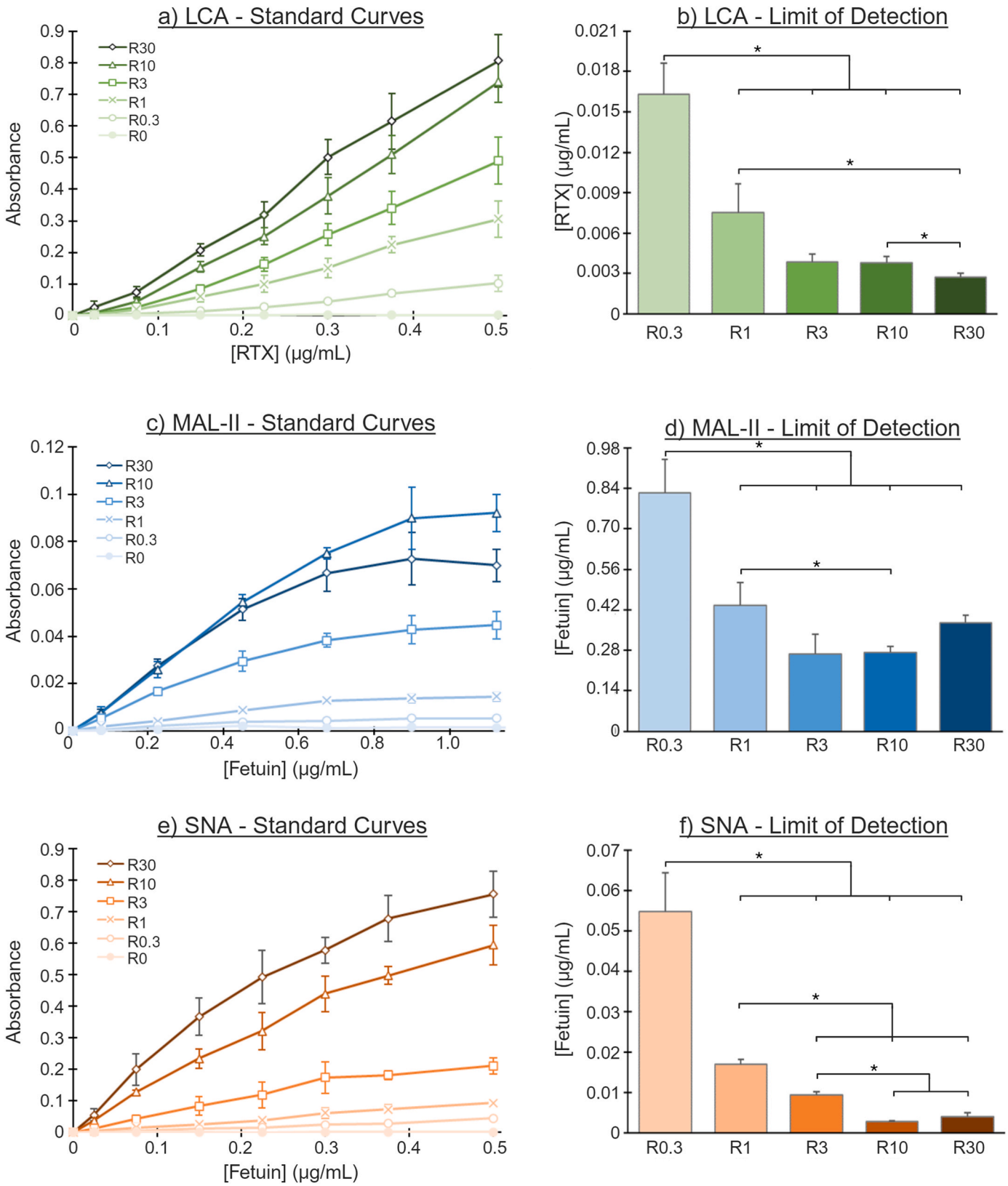

Fig. 6. Left: Standard curves of incubated glycoproteins constructed using a) LCA, c) MAL-II and e) SNA lectins at multiple biotin conjugation levels. Note that the connecting line between observation points serves as a visual aid and is not intended as a representative model (n = 3). Right: Limits of detection of the ELLA assay for b) LCA, d) MAL-II and f) SNA at the various biotin conjugation levels, calculated from the slopes of the standard curves according to the standard IUPAC method. Conditions were compared using a 1-tailed Student's T-test ($\alpha = 0.05$). Error bars represent standard deviations between replicates (n = 3).

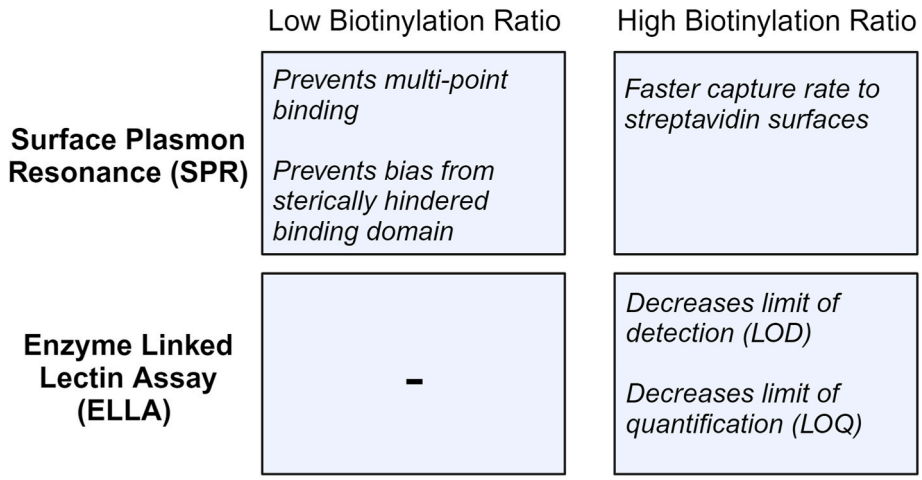

Fig. 7. Summary of the effects of the lectin biotinylation ratio for SPR and ELLA glycosylation assays.

While not explored in this work, the impact of biotinylation on streptavidin capture or recruitment would also depend upon the length and flexibility of the linker used between the lectin and the biotin. We theorize that longer linkers (i.e., more PEG repeats) would increase signal amplification in ELLA style assays, as a the bound lectin will have a greater reach and will be less limited by steric obstruction from already bound streptavidins. In the case of our SPR configuration, its thought that greater linker length will exascerbate the multi-point binding observed in high-biotinylation conditions. In effect, the PEG-linker length might be a viable avenue for further optimization of ligand biotinylation for SPR and ELLA style assays. The influence of PEG linker length on biotin-streptavidin interactions has been previously demonstrated in biosensor and cellular assays [41].

Crucially, this work has demonstrated that there is no "one size fits all" solution for the preparation of biotinylated lectins, and presents an experimental workflow for the optimization of lectin-based protein glycosylation assays via the modulation of the biotin conjugation ratio.

CRediT authorship contribution statement

Benjamin Serafin: Writing – original draft, Methodology, Formal analysis, Conceptualization. **Amine Kamen:** Writing – review & editing. **Gregory De Crescenzo:** Writing – review & editing, Supervision, Project administration, Funding acquisition, Conceptualization. **Olivier Henry:** Writing – review & editing, Supervision, Funding acquisition.

Statements

This work was supported by the Fonds de Recherche Nature et Technologies (FRQNT), grant number PR-300890, the Natural Sciences and Engineering Research Council of Canada (stipends allocated to Benjamin Serafin via the NSERC-CREATE PrEEmiuM program) (Nano-Bio Technology Platform) and its main funding partner, the Canada First Research Excellence Fund.

Declaration of competing interest

The authors declare that they have no known competing financial interests or personal relationships that could have appeared to influence the work reported in this paper.

Acknowledgements

We wish to thank Jimmy Gaudreault, Ilona Métayer and Sofiane Khan for producing rituximab used in this work, as well as Michel Gilbert for characterizing rituximab glycosylation by hydrophilic interaction chromatography (HILIC). The authors would also like to thank Benoit Liberelle and Jimmy Gaudreault for critical proofreading of the manuscript. All figures were created with BioRender.com.

Appendix A. Supplementary data

Supplementary data to this article can be found online at https://doi.org/10.1016/j.ab.2024.115693.

Data availability

Data will be made available on request.

References

[1] K.T. Schjoldager, Y. Narimatsu, H.J. Joshi, H. Clausen, Global view of human protein glycosylation pathways and functions, Nat. Rev. Mol. Cell Biol. 21 (2020) 729–749, https://doi.org/10.1038/s41580-020-00294-x.
[2] A. Varki, Biological roles of glycans, Glycobiology 27 (2017) 3–49, https://doi.org/10.1093/glycob/cww086.
[3] G.P. Subedi, A.W. Barb, The immunoglobulin g1 n-glycan composition affects binding to each low affinity fc gamma receptor, mAbs 8 (2016) 1512–1524, https://doi.org/10.1080/19420862.2016.1218586.
[4] C. Forest-Nault, J. Gaudreault, O. Henry, Y. Durocher, G. De Crescenzo, On the use of surface plasmon resonance biosensing to understand igg-fcgammar interactions, Int. J. Mol. Sci. 22 (2021), https://doi.org/10.3390/ijms22126616.
[5] K.-T. Shade, R. Anthony, Antibody glycosylation and inflammation, Antibodies 2 (2013) 392–414, https://doi.org/10.3390/antib2030392.
[6] Z. Wang, J. Zhu, H. Lu, Antibody glycosylation: impact on antibody drug characteristics and quality control, Appl. Microbiol. Biotechnol. 104 (2020) 1905–1914, https://doi.org/10.1007/s00253-020-10368-7.
[7] M. Butler, M. Spearman, The choice of mammalian cell host and possibilities for glycosylation engineering, Curr. Opin. Biotechnol. 30 (2014) 107–112, https://doi.org/10.1016/j.copbio.2014.06.010.
[8] W. Van Breedam, S. Pohlmann, H.W. Favoreel, R.J. de Groot, H.J. Nauwynck, Bitter-sweet symphony: glycan-lectin interactions in virus biology, FEMS Microbiol. Rev. 38 (2014) 598–632, https://doi.org/10.1111/1574-6976.12052.
[9] R. Thompson, A. Creavin, M. O'Connell, B. O'Connor, P. Clarke, Optimization of the enzyme-linked lectin assay for enhanced glycoprotein and glycoconjugate analysis, Anal. Biochem. 413 (2011) 114–122, https://doi.org/10.1016/j.ab.2011.02.013.
[10] A.M. Wu, E. Lisowska, M. Duk, Z. Yang, Lectins as tools in glycoconjugate research, Glycoconj. J. 26 (2009) 899–913, https://doi.org/10.1007/s10719-008-9119-7.
[11] J. Gaudreault, C. Forest-Nault, G. De Crescenzo, Y. Durocher, O. Henry, On the use of surface plasmon resonance-based biosensors for advanced bioprocess monitoring, Processes 9 (2021), https://doi.org/10.3390/pr9111996.
[12] K.J. Foley, E.S. Forzani, L. Joshi, N. Tao, Detection of lectin-glycan interaction using high resolution surface plasmon resonance, Analyst 133 (2008) 744–746, https://doi.org/10.1039/b719321a.
[13] C.F. Mandenius, R. Wang, A. Alden, G. Bergstrom, S. Thebault, C. Lutsch, et al., Monitoring of influenza virus hemagglutinin in process samples using weak affinity ligands and surface plasmon resonance, Anal. Chim. Acta 623 (2008) 66–75, https://doi.org/10.1016/j.aca.2008.06.005.
[14] G. Safina, B. Duran Iu, M. Alasel, B. Danielsson, Surface plasmon resonance for real-time study of lectin-carbohydrate interactions for the differentiation and

identification of glycoproteins, Talanta 84 (2011) 1284–1290, https://doi.org/10.1016/j.talanta.2011.01.030.
[15] J. Katrlík, R. Škrabana, D. Mislovičová, P. Gemeiner, Binding of d-mannose-containing glycoproteins to d-mannose-specific lectins studied by surface plasmon resonance, Colloids Surf. A Physicochem. Eng. Asp. 382 (2011) 198–202, https://doi.org/10.1016/j.colsurfa.2011.01.020.
[16] K. Matsumura, K. Higashida, H. Ishida, Y. Hata, K. Yamamoto, M. Shigeta, et al., Carbohydrate binding specificity of a fucose-specific lectin from aspergillus oryzae: a novel probe for core fucose, J. Biol. Chem. 282 (2007) 15700–15708, https://doi.org/10.1074/jbc.M701195200.
[17] P. Rouge, R. Culerrier, C. Granier, F. Rance, A. Barre, Characterization of ige-binding epitopes of peanut (arachis hypogaea) pna lectin allergen cross-reacting with other structurally related legume lectins, Mol. Immunol. 47 (2010) 2359–2366, https://doi.org/10.1016/j.molimm.2010.05.006.
[18] J. Katrlík, A. Holazová, I. Medovarská, I. Seilerová, P. Gemeiner, S. Bystrický, Spr biosensor chip based on mannan isolated from candida dubliniensis yeasts applied in immunization effectiveness testing, Sensor. Actuator. B Chem. 350 (2022), https://doi.org/10.1016/j.snb.2021.130883.
[19] L.S. Kelly, S. Birken, D. Puett, Determination of hyperglycosylated human chorionic gonadotropin produced by malignant gestational trophoblastic neoplasias and male germ cell tumors using a lectin-based immunoassay and surface plasmon resonance, Mol. Cell. Endocrinol. 260–262 (2007) 33–39, https://doi.org/10.1016/j.mce.2006.05.010.
[20] M.J. Linman, J.D. Taylor, H. Yu, X. Chen, Q. Cheng, Surface plasmon resonance study of protein-carbohydrate interactions using biotinylated sialosides, Anal. Chem. 80 (2008) 4007–4013, https://doi.org/10.1021/ac702566e.
[21] K. Nakamura, H. Sakagami, K. Asanuma-Date, N. Nagasawa, Y. Nakahara, H. Akiyama, et al., Immobilized glycosylated fmoc-amino acid for spr: comparative studies of lectin-binding to linear or biantennary dilacnac structures, Carbohydr. Res. 382 (2013) 77–85, https://doi.org/10.1016/j.carres.2013.10.003.
[22] J. Dorion-Thibaudeau, G. St-Laurent, C. Raymond, G. De Crescenzo, Y. Durocher, Biotinylation of the fcgamma receptor ectodomains by mammalian cell co-transfection: application to the development of a surface plasmon resonance-based assay, J. Mol. Recogn. 29 (2016) 60–69, https://doi.org/10.1002/jmr.2495.
[23] Y. Kim, S.O. Ho, N.R. Gassman, Y. Korlann, E.V. Landorf, F.R. Collart, et al., Efficient site-specific labeling of proteins via cysteines, Bioconjugate Chem. 19 (2008) 786–791, https://doi.org/10.1021/bc7002499.
[24] D. Rabuka, J.S. Rush, G.W. deHart, P. Wu, C.R. Bertozzi, Site-specific chemical protein conjugation using genetically encoded aldehyde tags, Nat. Protoc. 7 (2012) 1052–1067, https://doi.org/10.1038/nprot.2012.045.
[25] G. Papalia, D. Myszka, Exploring minimal biotinylation conditions for biosensor analysis using capture chips, Anal. Biochem. 403 (2010) 30–35, https://doi.org/10.1016/j.ab.2010.03.044.
[26] J.R. Litowski, R.S. Hodges, Designing heterodimeric two-stranded alpha-helical coiled-coils: the effect of chain length on protein folding, stability and specificity, J. Pept. Res. 58 (2001) 477–492, https://doi.org/10.1034/j.1399-3011.2001.10972.x.
[27] F. Cambay, O. Henry, Y. Durocher, G. De Crescenzo, Impact of n-glycosylation on fcgamma receptor/igg interactions: unravelling differences with an enhanced surface plasmon resonance biosensor assay based on coiled-coil interactions, mAbs 11 (2019) 435–452, https://doi.org/10.1080/19420862.2019.1581017.
[28] B. Liberelle, A. Merzouki, G. De Crescenzo, Immobilized carboxymethylated dextran coatings for enhanced elisa, J. Immunol. Methods 389 (2013) 38–44, https://doi.org/10.1016/j.jim.2012.12.007.
[29] M.L.S. Silva, Lectin biosensors in cancer glycan biomarker detection, Adv. Clin. Chem. 93 (2019) 1–61, https://doi.org/10.1016/bs.acc.2019.07.001.
[30] M. Degardin, J. Gaudreault, R. Oliverio, B. Serafin, C. Forest-Nault, B. Liberelle, et al., Grafting strategies of oxidation-prone coiled-coil peptides for protein capture in bioassays: impact of orientation and the oxidation state, ACS Omega 8 (2023) 28301–28313, https://doi.org/10.1021/acsomega.3c02172.
[31] G. De Crescenzo, J.R. Litowski, R.S. Hodges, M.D. O'Connor-McCourt, Real-time monitoring of the interactions of two-stranded de novo designed coiled-coils: Effect of chain length on the kinetic and thermodynamic constants of binding, Biochemistry 42 (2003) 1754–1763, https://doi.org/10.1021/bi0268450.
[32] E. Duverger, N. Lamerant-Fayel, N. Frison, M. Monsigny, Carbohydrate-lectin interactions assayed by spr, Methods Mol. Biol. 627 (2010) 157–178, https://doi.org/10.1007/978-1-60761-670-2_10.
[33] R. Loris, D. Van Overberge, M.H. Dao-Thi, F. Poortmans, N. Maene, L. Wyns, Structural analysis of two crystal forms of lentil lectin at 1.8 a resolution, Proteins 20 (1994) 330–346, https://doi.org/10.1002/prot.340200406.
[34] A. Imberty, C. Gautier, J. Lescar, S. Perez, L. Wyns, R. Loris, An unusual carbohydrate binding site revealed by the structures of two maackia amurensis lectins complexed with sialic acid-containing oligosaccharides, J. Biol. Chem. 275 (2000) 17541–17548, https://doi.org/10.1074/jbc.M000560200.
[35] E.J. Van Damme, A. Barre, P. Rouge, F. Van Leuven, W.J. Peumans, The neuac (alpha-2,6)-gal/galnac-binding lectin from elderberry (sambucus nigra) bark, a type-2 ribosome-inactivating protein with an unusual specificity and structure, Eur. J. Biochem. 235 (1996) 128–137, https://doi.org/10.1111/j.1432-1033.1996.00128.x.
[36] A. Di Vito, E. Reitano, L. Poggi, M. Iaboni, Biotin oligonucleotide labeling reactions: a method to assess their effectiveness and reproducibility, Anal. Biochem. 593 (2020) 113590, https://doi.org/10.1016/j.ab.2020.113590.
[37] Y.J. Li, L.J. Bi, X.E. Zhang, Y.F. Zhou, J.B. Zhang, Y.Y. Chen, et al., Reversible immobilization of proteins with streptavidin affinity tags on a surface plasmon resonance biosensor chip, Anal. Bioanal. Chem. 386 (2006) 1321–1326, https://doi.org/10.1007/s00216-006-0794-6.
[38] A. Erbas, F. Inci, The role of ligand rebinding and facilitated dissociation on the characterization of dissociation rates by surface plasmon resonance (spr) and benchmarking performance metrics, Methods Mol. Biol. 2385 (2022) 237–253, https://doi.org/10.1007/978-1-0716-1767-0_11.
[39] H. Ueda, H. Matsumoto, N. Takahashi, H. Ogawa, Psathyrella velutina mushroom lectin exhibits high affinity toward sialoglycoproteins possessing terminal n-acetylneuraminic acid alpha 2,3-linked to penultimate galactose residues of trisialyl n-glycans. Comparison with other sialic acid-specific lectins, J. Biol. Chem. 277 (2002) 24916–24925, https://doi.org/10.1074/jbc.M110727200.
[40] S.R. Haseley, P. Talaga, J.P. Kamerling, J.F. Vliegenthart, Characterization of the carbohydrate binding specificity and kinetic parameters of lectins by using surface plasmon resonance, Anal. Biochem. 274 (1999) 203–210, https://doi.org/10.1006/abio.1999.4277.
[41] Y. Teramura, K. Kuroyama, M. Takai, Influence of molecular weight of peg chain on interaction between streptavidin and biotin-peg-conjugated phospholipids studied with qcm-d, Acta Biomater. 30 (2016) 135–143, https://doi.org/10.1016/j.actbio.2015.11.003.